Ethanol extract of Cnidii Rhizoma ameliorates dextran sulfate sodium-induced ulcerative colitis by inhibiting JNK/NF-κB signaling

Yo-Han Han[1, †], Dae-Seung Kim[2, †], Ji-Ye Kee[1], Jung-Geon Mun[1], Hee-Dong Jeon[1], and Seung-Heon Hong[1]

[1]*Department of Oriental Pharmacy, College of Pharmacy, Wonkwang-Oriental Medicines Research Institute, Wonkwang University, 460 Iksandae-ro, Iksan, Jeonbuk 54538, Republic of Korea*

[2] *Pharmaceutical Safety Evaluation Division, Pharmaceutical Safety Bureau, Ministry of Food and Drug Safety, Cheongju, Korea.*

Correspondence to: Prof. Seung-Heon Hong, Department of Oriental Pharmacy, College of Pharmacy, Wonkwang-Oriental Medicines Research Institute, Wonkwang University, 460 Iksandae-ro, Iksan, Jeonbuk 54538, Republic of Korea. Tel: (+82) 63-850-6805, Fax: (+82) 63-843-3421, E-mail: jooklim@wku.ac.kr

[†]These authors contributed equally to this work.

Running title: Cnidii Rhizoma inhibit colitis via JNK/NF-κB signaling

 doi:10.20944/preprints201810.0144.v1

Abstract: In this study, dextran sulfate sodium (DSS)-induced *in vivo* model and LPS-stimulated *in vitro* model were used to confirm whether ethanol extract of Cnidii Rhizoma (EtCR) could ameliorate UC. EtCR improved symptoms of UC, including body weight loss, colon length shortening, disease activity index (DAI), and colon mucosal damage. In addition, EtCR decreased inflammatory mediators, including cyclooxygenase-2 (COX-2) and inducible nitric oxide synthase (iNOS), in colon tissue. To further confirm the UC improving mechanism, RAW 264.7 cells and HT29 human epithelial cells were used. EtCR reduced expression of inflammatory cytokines (IL-1β, TNF-α, and IL-6) and inflammatory mediators (nitric oxide and prostaglandin E_2) via JNK and NF-κB signaling pathway in RAW 264.7 cells. In addition, EtCR increased expression of trefoil factor 3 (TFF3), which is an epithelial cell protective factor, in HT29 cells. Taken together, our study suggests that EtCR has treatment effect on UC and can be a therapeutic agent.

Keywords: Cnidii Rhizoma; DSS; inflammation; NF-Kb; MAPKs; TFF3

 doi:10.20944/preprints201810.0144.v1

1. Introduction

Ulcerative colitis (UC) is a chronic and multifactorial inflammatory bowel disease (IBD), which is mainly occurred in the rectum and colon [1]. Nevertheless UC is not life-threatening in itself, it has been reported that chronic recurrence of UC could increase the risk of colorectal cancer, which is the third most common cancer in the world [2]. Several drugs such as aminosalicylic acid drugs, immune suppressor, and hormone agents have been used to treat UC. However, many people are still suffered from high recurrence rates of UC and side-effects of drugs [3]. Although the etiologies of UC and a lot of therapies have been studied, it is very difficult to treat because of recurrence and other unknown reasons.

Among the various causes of UC, pro-inflammatory cytokines, which are mainly secreted from macrophages, T cells and epithelial cells, is certainly thought as a crucial factor in the treatment of UC. Since recurrence of intestinal inflammation is related to an abnormal immune response, cytokines can be an important mediator to control the intestinal immune system [4]. In patients with UC, increased level of pro-inflammatory cytokines including IL-1β, IL-6, and TNF-α have observed and expression of these cytokines are regulated by many kinds of intracellular proteins [5,6]. Among them, mitogen-activated protein kinases (MAPKs), including extracellular signal-regulated kinases (ERKs), the c-Jun N-terminal kinases (JNKs) and the p38 MAPK, are participated in inflammatory response by producing inflammatory mediators [7]. These signaling pathways can regulate inflammation by converting extracellular stimuli into the intracellular signaling, which induce the expression of inflammation related genes [8].

Preprints (www.preprints.org) | NOT PEER-REVIEWED | Posted: 8 October 2018 doi:10.20944/preprints201810.0144.v1

Nuclear factor-kappa B (NF-κB), which is one of the downstream factor of MAPKs, is also crucial factor for treatment of UC. It has been reported that patients with UC show strongly activated NF-κB in colon tissues [9]. NF-κB is consisted of p50 and p65, which normally exist in cytoplasm with inhibitor of NF-κB (IκB) [10]. By extracellular stimuli, IκB is degraded and phosphorylated through ubiquitin/proteasome pathway, and then NF-κB is activated. Activated NF-κB is subsequently translocated into nucleus to bind with sequence of target genes [11]. Translocated NF-κB can regulate transcription of inflammation related genes, including cyclooxygenase-2 (COX-2) and inducible nitric oxide synthase (iNOS) [10]. COX-2, which is induced by inflammatory stimuli such as arthritis, asthma and IBD, contributes to not only the pain and swelling, but also converting of arachidonic acid to prostaglandin E_2 (PGE_2) [12-14]. Another downstream target of NF-κB is iNOS, which leads vasodilation of inflammatory cells easily [15]. iNOS is highly expressed in inflamed intestine mucosa and induces tissue damage by generating nitric oxide (NO) [16]. Therefore, suppressing NF-κB activation through MAPKs cascades is crucial for treating colitis.

Intestinal epithelium exhibits barrier function against luminal antigens. The intestinal epithelium is composed of a single epithelial cell layer. This layer is covered by mucus, which protects epithelial layer by distinguishing from mucosal bacteria [17]. To protect the intestine from bacterial infection and damage, epithelial cells secrete anti-microbial peptides into mucus [18]. Anti-microbial peptides are regulated by trefoil factor 3 (TFF3). TFF3, which is synthesized in the goblet cells of the small and large intestine, plays important roles in the protection and repair of epithelial surfaces, including the gastrointestinal tract [19].

In this study, we used rhizomes of *Cnidium officinale* Makino (Cinidii Rhizoma; CR). *Cnidium officinale* Makino is extensively cultivated and it has been used as medicine in East

 doi:10.20944/preprints201810.0144.v1

Asia [20]. Since CR contains 1-2 % of essential oil and several compounds, it has shown various pharmacological effects such as muscle relaxing, anti-tumor, anti-anemia, and anti-metastatic effects [21]. In particular, CR has been previously reported that improvement of blood circulation and anti-inflammatory effects [22]. However, there is no report on the therapeutic effect of CR on UC. Therefore, this study investigated that improvement effect of CR on colitis in *in vitro* and *in vivo*.

Preprints (www.preprints.org) | NOT PEER-REVIEWED | Posted: 8 October 2018 doi:10.20944/preprints201810.0144.v1

2. Results

2.1. EtCR Prevents Symptoms of Colitis in DSS-induced Colitis Mice

To estimate whether EtCR could inhibit progression of colitis, mice were administrated 5% DSS containing water with or without EtCR (50 mg/kg/day) and 5-ASA (50 mg/kg/day). As shown in Figure 1A, administration of DSS decreased body weight compared to control group. However, administration of EtCR inhibited weight loss similarly with 5-ASA, which is treatment drug of colitis. Also, the severity of colitis was presented by DAI score, which concerned other factors, including bleeding and diarrhea, as well as body weight. As shown in Figure 2B, DAI score of DSS group was steadily increased from day 5 to day 7. However, EtCR and 5-ASA treated groups showed better DAI score compared to only DSS-treated group. Since Shortening of colon length is closely related to the increased DAI scores [24], we measured colon length after sacrificing the mice. Similarly with DAI scores, EtCR and 5-ASA suppressed the reduction of colon length (Figure 1C,D). Furthermore, enlarged spleen was observed in DSS-treated mice, whereas administration of EtCR and 5-ASA decreased the size of spleen (Figure 1E). These results suggest that EtCR ameliorate DSS-induced colitis similar to 5-ASA.

2.2. EtCR Inhibits Colon Tissue Damages Induced by DSS

Since the administration of DSS induces colon tissue damages, including loss of epithelial layer, infiltration of inflammatory cells into the mucosa, and loss of goblet cells [25], we conducted H&E staining and alcian blue staining to confirm colonic protective effect of EtCR from DSS induced damages. As shown in Figure 2A, morphology alterations were

Preprints (www.preprints.org) | NOT PEER-REVIEWED | Posted: 8 October 2018 doi:10.20944/preprints201810.0144.v1

observed. Epithelial layer were almost eroded and crypt architecture were not found in DSS-treated colon tissue. In addition, infiltration of inflammatory cells was also shown in DSS-treated group. However, administration of EtCR and 5-ASA reduced not only damages of colon tissue, but also infiltration of inflammatory cells. To compare the degree of inflammation, we assessed the each group of H&E stained images and assigned scores. The scores indicated that administration of EtCR relieved severity of colitis. (Figure 2B). In addition, administration of EtCR inhibited the expression of COX-2 and iNOS, which are inflammatory factors increased by DSS (Figure 2E,F). Next, we confirmed goblet cells, which secrete a mucosal protective substance [26]. To stain goblet cells, alcian blue staining was conducted. As shown in Figure 2C, blue spots were well-shown in colon tissue of control group and it was seldom seen in DSS-treated group. In EtCR and 5-ASA-administrated groups, the blue stained cells were increased in colon tissues (Figure 2D). Furthermore, the TFF3 expression was recovered in EtCR and 5-ASA-administrated groups, compared with DSS-treated group (Figure 2E,G). Therefore, these results indicated that the EtCR could ameliorate colitis by protecting colon tissue.

2.3. EtCR Regulates LPS-stimulated Cytokine and Pro-Inflammatory Mediators in in vitro

To confirm whether EtCR could regulate inflammatory reaction, RAW 264.7 cells were used in this study. Since regulation of pro-inflammatory cytokines such as IL-1β, TNF-α and IL-6 is important in inflammation related diseases [27], we investigated whether EtCR has anti-inflammatory effects in LPS-stimulated RAW 264.7 cells. To determine the experimental dose of EtCR in RAW 264.7 cells, the cells were treated with 1, 10, and 100 μg/ml of EtCR. Since

Preprints (www.preprints.org) | NOT PEER-REVIEWED | Posted: 8 October 2018 doi:10.20944/preprints201810.0144.v1

EtCR did not show significant cytotoxicity up to 100 μg/ml of EtCR (Figure 3A), we used 100 μg/ml of EtCR as a highest concentration. As shown in Figure 3B-D, EtCR reduced the productions of IL-1β, TNF-α, and IL-6, compared to LPS treated group.

2.4. EtCR Decreases LPS-induced NO and PGE_2 by Suppressing iNOS and COX-2 in RAW 264.7 Cells

It has been reported that colon tissue damages induced by colitis is related to inflammatory mediators [28]. Thus, reducing the pro-inflammatory mediators as well as cytokines is also crucial for colitis. As shown in Figure 4A,B, pre-treatment of EtCR decreased levels of NO and PGE_2, which were elevated by LPS. In addition, we investigated expression levels of iNOS and COX-2, which produce NO and PGE_2, respectively. Similarly with the tendency of NO and PGE_2, EtCR reduced the expressions of iNOS and COX-2 (Figure 4C,D).

2.5. EtCR Reduces Inflammation Through NF-κB and MAPKs in RAW 264.7 Cells

NF-κB pathway regulates various inflammatory mediators. NF-κB exists in the cytoplasm in an inactive form with IκB. After inflammatory stimulation, IκB are phosphorylated and degraded. Continuously, NF-κB is translocated into the nucleus and leads to inflammatory responses [29]. As shown in Figure 5A,B, IκB in the cytoplasm was phosphorylated and degraded by LPS stimulation, which is an inflammatory stimulus. And then, NF-κB p65 was translocated into the nucleus. However, the treatment of EtCR suppressed this signaling pathway. In addition, the result of NF-κB binding assay showed that the EtCR

Preprints (www.preprints.org) | NOT PEER-REVIEWED | Posted: 8 October 2018 doi:10.20944/preprints201810.0144.v1

151 treatment effectively reduced the NF-κB binding activity, dose dependently (Figure 5C). It was
152 also reported that the NF-κB signaling is regulated by MAPKs, including ERK, JNK, and p38
153 [30]. As shown in Figure 5D and E, EtCR inhibited LPS-induced phosphorylation of JNK,
154 whereas ERK and p38 phosphorylation was not suppressed by EtCR. These results suggested
155 that EtCR inhibited the inflammatory response by inhibiting JNK and NF-κB signaling
156 pathway.

157

158 *2.6. EtCR Regulates TFF3 in HT 29 cells*

159 To confirm whether EtCR recovered the expression of TFF3, we used HT29 known as
160 colonic epithelial cells. Since HT29 cells show properties of pluripotent intestinal cells, they
161 are commonly used to investigate intestinal epithelial circumstance [31]. In our experiment,
162 TFF3 was fully expressed in HT29 cells, but this expression was inhibited by LPS treatment.
163 However, the treatment of EtCR increased TFF3 in both protein and mRNA level without
164 cytotoxicity (Figure 6). Thus, these results indicate that EtCR could ameliorate colitis by
165 protecting the epithelial cells of the intestine.

Preprints (www.preprints.org) | NOT PEER-REVIEWED | Posted: 8 October 2018 doi:10.20944/preprints201810.0144.v1

3. Discussion

UC and Crohn's disease (CD) are the two most common forms of IBD, which is characterized by a chronic inflammation of intestine. The etiologies of both diseases are unclear. However, main cause of these diseases is considered to multifactorial, including environmental factors such as smoking and western diet, the genetic factors and the intestinal flora [32]. Although the symptoms between UC and CD are similar in many parts, there are also slightly different. People suffering from UC have the abdominal pain in the left side of the abdomen, while suffering from CD have abdominal pain in their all abdomen. It has been known that CD is more severe than UC, but the incidence of CD is much lower than UC [33]. In addition, the treatment drugs of UC, including 5-ASA and glucocorticoids, occurred side-effects such as arthralgia, myalgia, headache, and abdominal pain [34]. Therefore, our study focused on UC rather than CD and suggested the new therapeutic agents of UC using natural products with few side effects.

EtCR is expected that could improve colitis through several research findings about EtCR. It has been reported that the health functional food containing CR improved TNBS-induced colitis and histological changes such as thickening, dilatation, ulceration, and infiltration [35]. In addition, CR had anti-inflammatory effect by reducing NO production in LPS-stimulated BV-2 microglia cell [36]. Despite these possibilities, there was no report on the effect of EtCR on UC. In this study, we confirmed whether EtCR can ameliorate UC, using DSS-induced colitis model. Since the symptoms, including weight loss, bloody stool, damages of colon tissue, colon shortening, and diarrhea, of this model are similar with human UC, it is often used to colitis experiment [37]. In our experiment, administration of DSS reduced body weight, which indicates DSS induced colitis. However, the administration of EtCR significantly inhibited

Preprints (www.preprints.org) | NOT PEER-REVIEWED | Posted: 8 October 2018 doi:10.20944/preprints201810.0144.v1

189 weight loss compared to DSS-treated group (Figure 1A). In addition, DAI scores and colon
190 shortening were improved by administration of EtCR (Figure 1B-D). It has been also reported
191 that the weight of spleen, which can produce inflammatory cytokines, was increased in DSS-
192 treated mice [38]. As shown in Figure 1E, the spleen weight was increased by DSS treatment,
193 whereas EtCR inhibited enlargement of spleen. In particular, EtCR exerted the similar
194 therapeutic effect as 5-ASA, which is a treatment drug of UC (Figure 1).

195 In normal condition, epithelial cell layer secretes protective substances to colon to maintain
196 colon condition. However, it cannot be secreted because of collapse of cell layer in colitis [39].
197 Therefore, symptoms such as diarrhea and bleeding are accompanied. Furthermore, the
198 weakened epithelial cell layer allows immune cells to infiltrate into the intestinal lumen [40].
199 In our experiment, administration of DSS almost eroded epithelial layer and crypt.
200 Inflammatory cell infiltration also found in colon tissue of DSS-treated group. However, EtCR
201 protected DSS-inducing mucosal erosion, disruption of intestinal crypts as well as
202 inflammatory cell infiltration (Figure 2A,B). We also confirmed goblet cell, which are
203 abundant in colon tissue and secreted protective mediators [41]. As shown in Figure 2C, blue
204 spots were well-shown in normal colon tissue, which is seldom seen in DSS-treated group.
205 However, the blue positive cells were increased in the colon tissue of 5-ASA group as well as
206 EtCR-administrated group (Figure 2C,D). Accordance with result of alcian blue staining, the
207 expression of TFF3, which is a constituent of mucus and is produced from goblet cell in large
208 intestine, was decreased in the colon tissue of DSS-treated group, but it was recovered by EtCR
209 administration (Figure 2E,G). These structural changes are known to be closely associated with
210 inflammatory reactions, and the inflammatory factors such as COX-2 and iNOS are found in
211 almost UC patients [42]. Similarly with clinical case, expressions of COX-2 and iNOS were

Preprints (www.preprints.org) | NOT PEER-REVIEWED | Posted: 8 October 2018 doi:10.20944/preprints201810.0144.v1

212 elevated in DSS-treated group. However, administration of EtCR reduced expression of COX-
213 2 and iNOS in colon tissue (Figure 2E,F). As a result, EtCR improved colitis in *in vivo*
214 experiment, and the therapeutic effect of EtCR is slightly lower than 5-ASA.

215 To further investigate the underlying anti-inflammatory mechanisms of EtCR, we
216 confirmed pro-inflammatory mediators in LPS-stimulated RAW 264.7 cells. The stimulated
217 macrophages secrete large amounts of IL-1, IL-6, and TNF-α [43]. Since the increased
218 expressions of pro-inflammatory cytokines such as IL-1, IL-6, IL-8, and TNF-α are also
219 detected in UC patients [5,6], this *in vitro* model was used to investigate the anti-inflammatory
220 mechanism of EtCR. Falcarindiol, 6-hydroxy-7-methoxy-dihydroligustilide, ligustilidiol, and
221 senkyunolide H were isolated from methanol extract of CR and they showed inhibitory effects
222 on iNOS and COX-2 expresion in LPS-stimulated RAW 264.7 cells [44]. In our experiment,
223 LPS-stimulated RAW 264.7 cells secreted pro-inflammatory cytokines, but EtCR treatment
224 reduced the production of IL-1β, TNF-α, and IL-6 (Figure 3). Similar to *in vivo* results, the
225 expressions of iNOS and COX-2 were inhibited by EtCR. In addition, the production of NO
226 and PGE_2, which are produced by iNOS and COX-2, were also decreased by EtCR (Figure 4).
227 Thus, it is quite convincing that therapeutic effect on UC may come from anti-inflammatory
228 properties of EtCR.

229 Ethanol extract of *Cnidium officinale* Makino showed anti-inflammatory effects by
230 blocking NF-κB pathway in BV2 microglial cells [45]. Therefore, we confirmed whether EtCR
231 can regulate anti-inflammatory factors via NF-κB pathway in RAW 264.7 cells. NF-κB is plays
232 a critical role in the immune system, which controls the expression of enzymes and cytokines
233 during inflammatory responses [46]. In normal condition, NF-κB binds to its inhibitor IκB, and
234 could not translocate to the nucleus. Once IκB is phosphorylated by IKK, IκB is degraded and

Preprints (www.preprints.org) | NOT PEER-REVIEWED | Posted: 8 October 2018 doi:10.20944/preprints201810.0144.v1

NF-κB undergoes nuclear translocation, and it triggers the expression of pro-inflammatory genes [47]. Therefore, we investigated IκB phosphorylation and NF-κB translocation. Based on our results, LPS treatment induced phosphorylation of IκB and nuclear translocation of NF-κB, but EtCR decreased IκB phosphorylation and NF-κB translocation (Figure 5A,B). Furthermore, the binding NF-κB to the nucleus induced by LPS was inhibited by EtCR (Figure 5C). Moreover, we confirmed expression of MAPKs in EtCR-treated cells, because the activation of MAPKs have been known to regulate NF-κB as an upstream factors [48]. In this study, EtCR treatment attenuated LPS-induced phosphorylation of JNK, but not ERK and p38 (Figure 5D,E). These results showed that EtCR inhibited the expression of inflammatory mediators through JNK and NF-κB pathway. From this result, the inhibitory effect of EtCR on DSS-induced colitis was considered to the regulation of JNK and NF-κB signaling pathway.

To confirm expression level of TFF3, LPS-stimulated human epithelial cell line HT29 was used. Once mucosal layer is depleted, epithelial cells are exposed directly to luminal contents such as bacteria and their metabolites [49]. In this experiment, LPS was used as an inflammatory stimulator to intestinal epithelial cells. It has been known that LPS reduces TFF3 expression by activating NF-κB in HT29 cells [50]. Consistent with this report, LPS inhibited the expression of TFF3, but treatment of EtCR on HT29 cells recovered the expression of TFF3 (Figure 6).

Preprints (www.preprints.org) | NOT PEER-REVIEWED | Posted: 8 October 2018 doi:10.20944/preprints201810.0144.v1

4. Experimental Section

4.1. Reagents and Antibodies

5-aminosalicylic acid (ASA), dimethyl sulfoxide (DMSO), triton-X, alcian blue, eosin, neutral buffered formalin, and lipopolysaccharides (LPS) were obtained from Sigma-Aldrich (St. Louis, MO. USA). Skim milk was purchased from BD Difco Laboratories (Detroit, MI, USA). Gill's hematoxylin V was purchased from Muto Pure Chemicals (Tokyo, Japan). Xylene was purchased from Dae-Jung chemicals (Siheung, Republic of Korea). Dextran sulfate sodium (DSS) (mol wt: 36,000 – 50,000) was purchased from MP Biomedicals (Solon, OH, USA). Dulbecco's Modified Eagles Medium (DMEM), fetal bovine serum (FBS), and phosphate-buffered saline (PBS) were obtained from WelGENE (Gyeongsan, Republic of Korea). The anti-rabbit IgG, anti-mouse IgG, and anti-goat IgG antibodies were purchased from Jackson ImmunoResearch Laboratories (West Grove, PA, USA). Mouse TNF-α, IL-1β, and IL-6 enzyme-linked immunosorbent assay (ELISA) kits were purchased from BD Biosciences (Mountain View, CA). Antibodies against COX-2, iNOS, p38, ERK, JNK, NF-κB, PCNA, IκB, phospho-IκB, and glyceraldehyde 3-phosphate dehydrogenase (GAPDH) were purchased from Santa Cruz Biotechnology (Santa Cruz, CA, USA). Phospho-p38, phospho-ERK, and phospho-JNK were purchased from Cell Signaling Technology, Inc. (Danvers, MA, United States). TFF3 antibody was purchased from Invitrogen (Carlsbad, CA, USA).

4.2. Ethanol Extract of CR (EtCR)

CR was purchased from Omniherb (Uiseong, Republic of Korea). EtCR was obtained by extracting dried 100 g of CR in 1 liter of 70% ethanol for approximately 3 h in heating mantle

Preprints (www.preprints.org) | NOT PEER-REVIEWED | Posted: 8 October 2018 doi:10.20944/preprints201810.0144.v1

with reflux condenser. After eliminating solvent with rotary evaporator under reduced pressure (Rotary evaporator Model NE-1, Tokyo, Japan), the remnant was filtered and lyophilized (Freeze dryer FD-1, Japan) at -56°C and 9 mm Torr to acquire herbal sample. The yield from the starting material was about 5%. The obtained sample was diluted using ethanol and then filtered through a 0.22-μm syringe filter.

4.3. Induction of DSS-induced Colitis in Mouse Model

Female BALB/c mice (6 weeks old) were purchased from Samtaco Science (Osan, Republic of Korea). Before inducing colitis, mice were maintained in experimental environment (22 ± 2°C under a 12-h light/dark cycle) for one week. To induce colitis in mice, drinking water containing 5% (w/v) DSS is given for seven days. Mice were randomly divided into four groups (n = 8): the control group were fed drinking water without DSS, the DSS group fed drinking water with DSS, the EtCR group fed drinking water with DSS and oral administration of EtCR (50 mg/kg), and the 5-ASA group fed drinking water with DSS and oral administration of 5-ASA (50 mg/kg; a reference drug). EtCR and 5-ASA were suspended in 0.3% CMC water. EtCR and 5-ASA were orally administered daily during 7 days. Control group and DSS group were administered with the same volume of water. Drugs were simultaneously administrated with the DSS treatment. After 7 days, mice were sacrificed and colon length and spleen weight were measured. All experiments were carried out in accordance with the regulations issued by the Institutional Review Board of Wonkwang University (WKU15-82).

Preprints (www.preprints.org) | NOT PEER-REVIEWED | Posted: 8 October 2018 doi:10.20944/preprints201810.0144.v1

296

297 *4.4. Disease Activity Index (DAI)*

298 DAI was calculated by scoring weight loss, diarrhea, and rectal bleeding. Each score was
299 assessed as shown in Table 1, which was described by Murthy *et al* [23]. Briefly, weight loss
300 was determined as the difference between initial and final weights. Diarrhea was evaluated to
301 degree of the fecal pellet formation. Rectal bleeding was assessed based on the presence of
302 visible blood. After calculation using the following formula, DAI were recorded: DAI =
303 {(weight loss score) + (diarrhea score) + (rectal bleeding score)}/2.

304

305 *4.5. Colon Tissue Staining and Evaluation of Colitis Severity*

306 All resected colon tissues were fixed in 10% neutral buffered formalin for 24 hours. After
307 paraffin embedding, samples were sectioned to 5 μm. The sections were stained with
308 hematoxylin and eosin (H&E) and Alcian blue/Nuclear Fast Red. Each stained images were
309 captured by Leica Application Suite MicroSoftware (Leica Microsystems Inc, IL, USA).
310 Histological scores were based on epithelium and infiltration. The damages of epithelium were
311 determined as follows: Normal morphology; 0, loss of goblet cells; 1, loss of goblet cells in
312 large areas; 2, loss of crypts; 3, loss of crypts in large areas; 4. Infiltration of mucosal immune
313 cell were determined as follows: no infiltrate; 0, infiltrate around the crypt basis; 1, infiltrate
314 reaching the L. muscularis mucosae; 2 extensive infiltration reaching the L. muscularis
315 mucosae and thickening of the mucosa with abundant edema; 3, infiltration of the L.
316 submucosa; 4. The total histological score was given as sum of epithelium and infiltration.

Preprints (www.preprints.org) | NOT PEER-REVIEWED | Posted: 8 October 2018 doi:10.20944/preprints201810.0144.v1

317 Alcian Blue positive cells were counted in ten random areas using microscope (Leica, Wetzlar,
318 Germany).

319

320 *4.6. Cell Culture*

321 RAW 264.7 cells and HT29 cells were purchased in Korean cell line bank (Seoul, Republic
322 of Korea). The cells were cultured at 37°C under 5% CO_2 in 10% FBS/DMEM supplemented
323 with 1% penicillin/streptomycin. The cells were pretreated with 1, 10, and 100 μg/mL of EtCR
324 for 1 h, and then stimulated with 200 ng/mL of LPS for 24 h. EtCR was diluted by ethanol
325 whose final concentration was below 0.1%.

326

327 *4.7. Cell Viability*

328 Cell viability was determined by 3-(4,5-dimethylthiazol-2-yl)-diphenyl-
329 tetrazoliumbromide (MTT) assay. Briefly, RAW 264.7 and HT29 cells were seeded in 24-well
330 plates at 3×10^5 cells/well and the cells were incubated with various concentrations of EtCR.
331 After 24 h, 5 mg/mL of MTT solution was treated for 4 h in incubator. After washing off the
332 supernatant, the insoluble formazan product was dissolved in DMSO and loaded into 96-well
333 microplate. The absorbance was measured at 540 nm with a VERSA max microplate reader
334 (Molecular Devices, Sunnyvale, CA, USA).

335

336 *4.8. Cytokine Assay*

Preprints (www.preprints.org) | NOT PEER-REVIEWED | Posted: 8 October 2018 doi:10.20944/preprints201810.0144.v1

To confirm the cytokine production from EtCR and LPS treated cells, 3×10^5 cells were seeded into 24-well plates. Various concentrations of EtCR were pretreated for 1 h prior to 24 h treatment with 200 ng/mL LPS. And then, cytokines, including IL-1β, IL-6, and TNF-α, were confirmed using supernatant. The production levels of IL-1β, IL-6, and TNF-α were confirmed using ELISA kits, according to the manufacturer's instructions.

4.9. NO Assay

RAW 264.7 cells were seeded (5×10^5 cell/well) and incubated with EtCR and LPS as already described in our study. To measure the NO content in the culture supernatant, Griess Reagent (1% sulfanilamide/0.1% N-(1-naphthyl)-ethylenediamine dihydrochloride/2.5% H_3PO_4) was used. Equal volume of supernatant and Griess reagent were incubated for 10 minutes at room temperature. The NO^{2-} level in supernatant was determined using sodium nitrite as a standard and the absorbance was measured by a microplate reader at a wavelength of 540 nm.

4.10. PGE_2 Assay

To measure the amount of PGE_2, 5×10^5 of RAW 264.7 cells were seeded in 24-well plated and treated with EtCR and LPS. The PGE_2 concentration was calculated using a PGE_2 ELISA kit (Enzo Life Sciences, USA) according to the manufacturer's directions.

4.11. Western Blot Analysis

Preprints (www.preprints.org) | NOT PEER-REVIEWED | Posted: 8 October 2018 doi:10.20944/preprints201810.0144.v1

358 RAW 264.7 cells (5×10^6 cell/well) and HT29 cells (5×10^6 cell/well) were cultured in 6
359 cm dish. EtCR and LPS were treated as already described in our study. The cells were washed
360 with PBS and then lysed by lysis buffer (iNtRON Biotech, Seongnam, Republic of Korea).
361 Nuclear extracts were isolated using the NE-PER Nuclear and Cytoplasmic Extraction
362 Reagents kit (Thermo Fisher Scientific, Waltham, MA, United States) according to the
363 manufacturer's protocols. The cell lysates were mixed with an equal volume of 2 × SDS sample
364 buffer and boiled at 95 °C for 5 min. The samples were loaded and separated by SDS-page gels.
365 After electrophoresis, the proteins were transferred onto PVDF membranes and divided
366 according to the size of each target proteins. The membranes were blocked by 5% skim milk
367 for 2 hours and incubated with primary antibodies overnight at 4°C. After washing the
368 membrane with 0.1% PBST 5 times, the membranes were incubated with horseradish
369 peroxidase-conjugated secondary Abs for 1 hour. The membranes were washed with PBST 5
370 more times and the protein bands were visualized by ECL solution. Images were captured using
371 the FluorChem E system (ProteinSimple, San Jose, CA, USA).

372

373 *4.12. NF-κB Binding Assay*

374 The nuclear extract was incubated with an immobilized oligonucleotide on a 96-well plate
375 containing a specific NF-κB binding site and detected by a specific p65 NF-κB subunit ELISA
376 kit (Affymetrix, Santa Clara, CA, USA), according to the manufacturer's instructions.

377

378 *4.13. Real-time RT-PCR*

Preprints (www.preprints.org) | NOT PEER-REVIEWED | Posted: 8 October 2018 doi:10.20944/preprints201810.0144.v1

379 Total RNA was extracted from the cells using an Easy-Blue total RNA extraction kit
380 (iNtRON Biotech, Republic of Korea) according to the manufacturer's instructions. First-
381 strand cDNA was reverse-transcribed using 2 μg of RNA and an Accupower®RT PreMix
382 (Bioneer, Daejeon, Republic of Korea). The primers of TFF3 and GAPDH were used for real-
383 time PCR analysis. Real-time PCR was performed using a Power SYBR® Green PCR Master
384 Mix and a StepOneplus Real-Time PCR System (Applied Biosystems, Foster City, CA, USA).
385 All data were normalized to GAPDH mRNA. Sequences of the primers used for human genes
386 were as follows: TFF3, 5'-CTCCAGCTCTGCTGAGGAGT-3', 5'-
387 CAGGGATCCTGGAGTCAAA-3'; GAPDH, 5'-CGGAGTCAACGGATTTGGTCGTAT-3',
388 5'-AGCCTTCTCCATGGTGGTGAAGAC-3'

389

390 *4.14. Statistical analysis*

391 The results are expressed as the mean ± S.D. of independent experiments. Statistical
392 evaluations were performed by a one-way analysis of variance (ANOVA) with Tukey's
393 multiple comparison test. All statistical analyses were computed by SPSS statistical analysis
394 software version 12.0 (SPSS Inc., Chicago, IL, United States). Values of $p < 0.05$ were
395 considered to represent significant differences.

396

397 **5. Conclusions**

398 Our study demonstrated that EtCR ameliorated UC in DSS-induced mice and protected
399 epithelial cell layer by recovering expression of TFF3. EtCR inhibited inflammatory factors in

 doi:10.20944/preprints201810.0144.v1

400 colon tissue. In *in vitro* experiment, EtCR inhibited inflammatory factors, including iNOS and
401 COX-2, through JNK and NF-κB pathway. In addition, EtCR regulated TFF3 in colon
402 epithelial cells. EtCR is expected to have fewer side effects because it is derived from natural
403 products. Based on these results, EtCR could be therapeutic agent and alternative supplement
404 for UC.

405 **Acknowledgments:**This paper was supported by Wonkwang University in 2017.

406

407 **Author Contributions:** Y.-H.H. participated in the study design, analyzed the data and
408 wrote the manuscript. D.-S.K. carried out the experiments. J.-Y.K. provided technical and
409 material support. J.-G.M., and H.-D.J. performed the experiments and analyzed the data. S.-
410 H.H. designed and supervised the study, including editing of the manuscript. All authors
411 contributed to and have approved the final manuscript.

412

413 **Conflicts of Interest:** The authors declare no conflict of interest.

 doi:10.20944/preprints201810.0144.v1

References

1. Morrison, G.; Headon, B.; Gibson, P. Update in inflammatory bowel disease. *Aust. Fam. Physician* **2009**, 38, 956-961.

2. Bibi, S.; Du, M.; Zhu, M.J. Dietary Red Raspberry Reduces Colorectal Inflammation and Carcinogenic Risk in Mice with Dextran Sulfate Sodium-Induced Colitis. *J. Nutr.* **2018**, doi: 10.1093/jn/nxy007.

3. Wang, L.; Yu, Z.; Wei, C.; Zhang, L.; Song, H.; Chen, B.; Yang, Q. Huaier aqueous extract protects against dextran sulfate sodium-induced experimental colitis in mice by inhibiting NLRP3 inflammasome activation. *Oncotarget* **2017**, 8, 32937-32945.

4. Sanchez-Munoz, F.; Dominguez-Lopez, A.; Yamamoto-Furusho, J.K. Role of cytokines in inflammatory bowel disease. *World J. Gastroenterol.* **2008**, 14, 4280-4288.

5. Sartor, R.B. Cytokines in intestinal inflammation: pathophysiological and clinical considerations. *Gastroenterology* **1994**, 106, 533-539.

6. Fiocchi, C. Inflammatory bowel disease: etiology and pathogenesis. *Gastroenterology* **1998**, 115, 182-205.

7. Sun, P.; Zhou, K.; Wang, S.; Li, P.; Chen, S.; Lin, G.; Zhao, Y.; Wang, T. Involvement of MAPK/NF-κB signaling in the activation of the cholinergic anti-inflammatory pathway in experimental colitis by chronic vagus nerve stimulation. *PLoS One* **2013**, 8, e69424.

8. Huang, P.; Han, J.; Hui, L. MAPK signaling in inflammation-associated cancer development. *Protein Cell* **2010**, 1, 218-226.

 doi:10.20944/preprints201810.0144.v1

9. Atreya, I.; Atreya, R.; Neurath, M.F. NF-kappaB in inflammatory bowel disease. *J. Intern. Med.* **2008**, 263, 591-596.

10. Li, Q.; Verma, I.M. NF-kappaB regulation in the immune system. *Nat. Rev. Immunol.* **2002**, 2, 725-734.

11. Neurath, M.F.; Becker, C.; Barbulescu, K. Role of NF-kappaB in immune and inflammatory responses in the gut. *Gut* **1998**, 43, 856-860.

12. Pang, L.; Pitt, A.; Petkova, A.J.; Knox, D. The COX-1/COX-2 balance in asthma. *Clin. Exp. Allergy* **1998**, 28, 1050-1058.

13. Siegle, I.; Klein, T.; Backman, J.T.; Saal, J.G.; Nüsing, R.M.; Fritz, P. Expression of cyclooxygenase 1 and cyclooxygenase 2 in human synovial tissue: differential elevation of cyclooxygenase 2 in inflammatory joint diseases. *Arthritis Rheum.* **1998**, 41, 122-129.

14. McCartney, S.A.; Mitchell, J.A.; Fairclough, P.D.; Farthing, M.J.; Warner, T.D. Selective COX-2 inhibitors and human inflammatory bowel disease. *Aliment. Pharmacol. Ther.* **1999**, 13, 1115-1117,

15. Zhao, H.; Zhao, M.; Wang, Y.; Li, F.; Zhang, Z. Glycyrrhizic Acid Attenuates Sepsis-Induced Acute Kidney Injury by Inhibiting NF-κB Signaling Pathway. *Evid. Based Complement. Alternat. Med.* **2016**, 2016, 8219287.

16. Lauritsen, K.; Laursen, L.S.; Bukhave, K.; Rask-Madsen, J. In vivo profiles of eicosanoids in ulcerative colitis, Crohn's colitis, and Clostridium difficile colitis. *Gastroenterology* **1988**, 95, 11-17.

17. Swidsinski, A.; Ladhoff, A.; Pernthaler, A.; Swidsinski, S.; Loening-Baucke, V.; Ortner,

 doi:10.20944/preprints201810.0144.v1

455 M.; Weber, J.; Hoffmann, U.; Schreiber, S.; Dietel, M.; Lochs, H. Mucosal flora in
456 inflammatory bowel disease. *Gastroenterology* **2002**, 122, 44-54,

457 18. Macpherson, A.J.; Uhr, T. Induction of protective IgA by intestinal dendritic cells carrying
458 commensal bacteria. *Science* **2004**, 303, 1662-1665.

459 19. Podolsky, D.K.; Lynch-Devaney, K.; Stow, J.L.; Oates, P.; Murgue, B.; DeBeaumont, M.;
460 Sands, B.E.; Mahida, Y.R. Identification of human intestinal trefoil factor. Goblet cell-
461 specific expression of a peptide targeted for apical secretion. *J. Biol. Chem.* **1993**, 268,
462 6694-6702.

463 20. Ramalingam, M.; Park, Y.K. Free radical scavenging activities of Cnidium officinale
464 Makino and Ligusticum chuanxiong Hort. methanolic extracts. *Pharmacogn. Mag.* **2010**,
465 6, 323-330.

466 21. Onishi, Y.; Yamaura, T.; Tauchi, K.; Sakamoto, T.; Tsukada, K.; Nunome, S.; Komatsu, Y.;
467 Saiki, I. Expression of the anti-metastatic effect induced by Juzen-taiho-to is based on the
468 content of Shimotsu-to constituents. *Biol. Pharm. Bull.* **1998**, 21, 761-765.

469 22. Wang, J.D.; Narui, T.; Kurata, H.; Takeuchi, K.; Hashimoto, T.; Okuyama, T.
470 Hematological studies on naturally occurring substances. II. Effects of animal crude drugs
471 on blood coagulation and fibrinolysis systems. *Chem. Pharm. Bull. (Tokyo)* **1989**, 37,
472 2236- 2238,

473 23. Murthy, S.N.; Cooper, H.S.; Shim, H.; Shah, R.S.; Ibrahim, S.A.; Sedergran, D.J.
474 Treatment of dextran sulfate sodium-induced murine colitis by intracolonic cyclosporin.
475 *Dig. Dis. Sci.* **1993**, 38, 1722-1734.

 doi:10.20944/preprints201810.0144.v1

476 24. Chen, M.; Gao, L.; Chen, P.; Feng, D.; Jiang, Y.; Chang, Y.; Jin, J.; Chu, F.F.; Gao, Q.
477 Serotonin-Exacerbated DSS-Induced Colitis Is Associated with Increase in MMP-3 and
478 MMP-9 Expression in the Mouse Colon. *Mediators Inflamm.* **2016**, 2016, 5359768.

479 25. Kim, J.J.; Shajib, M.S.; Manocha, M.M.; Khan, W.I. Investigating intestinal inflammation
480 in DSS-induced model of IBD. *J. Vis. Exp.* **2012**, 60, pii: 3678.

481 26. Pelaseyed, T.; Bergström, J.H.; Gustafsson, J.K.; Ermund, A.; Birchenough, G.M.; Schütte,
482 A.; van der Post, S.; Svensson, F.; Rodríguez-Piñeiro, A.M.; Nyström, E.E.; Wising, C.;
483 Johansson, M.E.; Hansson, G.C. The mucus and mucins of the goblet cells and enterocytes
484 provide the first defense line of the gastrointestinal tract and interact with the immune
485 system. *Immunol. Rev.* **2014**, 260, 8-20.

486 27. Qian, Z.; Wu, Z.; Huang, L.; Qiu, H.; Wang, L.; Li, L.; Yao, L.; Kang, K.; Qu, J.; Wu, Y.;
487 Luo, J.; Liu, J.J.; Yang, Y.; Yang, W.; Gou, D. Mulberry fruit prevents LPS-induced NF-
488 κB/pERK/MAPK signals in macrophages and suppresses acute colitis and colorectal
489 tumorigenesis in mice. *Sci. Rep.* **2015**, 5, 17348.

490 28. Stevceva, L.; Pavli, P.; Husband, A.J.; Doe, W.F. The inflammatory infiltrate in the acute
491 stage of the dextran sulphate sodium induced colitis: B cell response differs depending on
492 the percentage of DSS used to induce it. *B.M.C. Clin. Pathol.* **2001**, 1, 3.

493 29. Roman-Blas, J.A.; Jimenez, S.A. NF-kappaB as a potential therapeutic target in
494 osteoarthritis and rheumatoid arthritis. Osteoarthritis Cartilage 2006, **149**, 839-848.

495 30. Yeom, M.; Kim, J.H.; Min, J.H.; Hwang, M.K.; Jung, H.S.; Sohn, Y. Xanthii fructus
496 inhibits inflammatory responses in LPS-stimulated RAW 264.7 macrophages through

497 suppressing NF-κB and JNK/p38 MAPK. *J. Ethnopharmacol.* **2015**, 176, 394-401.

498 31. Jang, H.; Park, S.; Lee, J.; Myung, J.K.; Jang, W.S.; Lee, S.J.; Myung, H.; Lee, C.; Kim,
499 H.; Lee, S.S.; Jin, Y.W.; Shim, S. Rebamipide alleviates radiation-induced colitis through
500 improvement of goblet cell differentiation in mice. *J. Gastroenterol. Hepatol.* **2018**, 33,
501 878-886.

502 32. Knights, D.; Lassen, K.G.; Xavier, R.J. Advances in inflammatory bowel disease
503 pathogenesis: linking host genetics and the microbiome. *Gut* **2013**, 62, 1505-1510.

504 33. Gohil, K.; Carramusa, B. Ulcerative colitis and Crohn's disease. *P.T.* **2014**, 39, 576-577.

505 34. Ye, B.; van Langenberg, D.R. Mesalazine preparations for the treatment of ulcerative
506 colitis: Are all created equal? *World J. Gastrointest. Pharmacol. Ther.* **2015**, 6, 137-144.

507 35. Jo, S.K.; Lee, H.J.; Kim, S.R.; Kim, J.C.; Bae, C.S.; Jung, U.; Park, H.R.; Jang, J.S.; Kim,
508 S.H. Antiinflammatory activity of an herbal preparation (HemoHIM) in rats. *Phytother.*
509 *Res.* **2007**, 21, 625-628.

510 36. Kim, J.M.; Son, D.; Lee, P.; Lee, K.J.; Kim, H.; Kim, S.Y. Ethyl acetate soluble fraction
511 of Cnidium officinale MAKINO inhibits neuronal cell death by reduction of excessive
512 nitric oxide production in lipopolysaccharide-treated rat hippocampal slice cultures and
513 microglia cells. *J. Pharmacol. Sci.* **2003**, 92: 74-78.

514 37. Kiesler, P.; Fuss, I.J.; Strober, W. Experimental Models of Inflammatory Bowel Diseases.
515 *Cell. Mol. Gastroenterol. Hepatol.* **2015**, 1, 154-170.

516 38. Chen, L.; Zhou, Z.; Yang, Y.; Chen, N.; Xiang, H. Therapeutic effect of imiquimod on
517 dextran sulfate sodium-induced ulcerative colitis in mice. *PLoS One* **2017**, 12, e0186138.

518 39. Oehlers, S.H.; Flores, M.V.; Hall, C.J.; Crosier, K.E.; Crosier, P.S. Retinoic acid suppresses
519 intestinal mucus production and exacerbates experimental enterocolitis. *Dis. Model. Mech.*
520 **2012**, 5, 457-467.

521 40. Elson, C.O.; Cong, Y.; McCracken, V.J.; Dimmitt, R.A.; Lorenz, R.G.; Weaver, C.T.
522 Experimental models of inflammatory bowel disease reveal innate, adaptive, and
523 regulatory mechanisms of host dialogue with the microbiota. *Immunol. Rev.* **2005**, 206,
524 260-276.

525 41. Bergstrom, K.S.; Guttman, J.A.; Rumi, M.; Ma, C.; Bouzari, S.; Khan, M.A.; Gibson, D.L.;
526 Vogl, A.W.; Vallance, B.A. Modulation of intestinal goblet cell function during infection
527 by an attaching and effacing bacterial pathogen. *Infect. Immun.* **2008**, 76, 796-811.

528 42. Wang, D.; Dubois, R.N. The role of COX-2 in intestinal inflammation and colorectal
529 cancer. *Oncogene* **2010**, 29, 781-788.

530 43. Neurath, M.F.; Weigmann, B.; Finotto, S.; Glickman, J.; Nieuwenhuis, E.; Iijima, H.;
531 Mizoguchi, A.; Mizoguchi, E.; Mudter, J.; Galle, P.R.; Bhan, A.; Autschbach, F.; Sullivan,
532 B.M.; Szabo, S.J.; Glimcher, L.H.; Blumberg, R.S. The transcription factor T-bet regulates
533 mucosal T cell activation in experimental colitis and Crohn's disease. *J. Exp. Med.* **2002**,
534 195, 1129-1143.

535 44. Bae, K.E.; Choi, Y.W.; Kim, S.T.; Kim, Y.K. Components of rhizome extract of Cnidium
536 officinale Makino and their in vitro biological effects. *Molecules* **2011**, 16, 8833-8847.

537 45. Lee, S.H.; Lee, J.H.; Oh, E.Y.; Kim, G.Y.; Choi, B.T.; Kim, C.; Choi, Y.H. Ethanol extract
538 of Cnidium officinale exhibits anti-inflammatory effects in BV2 microglial cells by

 doi:10.20944/preprints201810.0144.v1

539 suppressing NF-κB nuclear translocation and the activation of the PI3K/Akt signaling
540 pathway. *Int. J. Mol. Med.* **2013**, 32, 876-882.

541 46. Kim, J.B.; Han, A.R.; Park, E.Y.; Kim, J.Y.; Cho, W.; Lee, J.; Seo E.K.; Lee, K.T. Inhibition
542 of LPS-induced iNOS, COX-2 and cytokines expression by poncirin through the NF-
543 kappaB inactivation in RAW 264.7 macrophage cells. *Biol. Pharm. Bull.* **2007**, 30, 2345-
544 2351.

545 47. Baeuerle, P.A.; Baltimore, D. NF-kappa B: ten years after. *Cell* **1996**, 87, 13-20.

546 48. Dong, Z.W.; Chen, J.; Ruan, Y.C.; Zhou, T.; Chen, Y.; Chen, Y.; Tsang, L.L.; Chan, H.C.;
547 Peng, Y.Z. CFTR-regulated MAPK/NF-κB signaling in pulmonary inflammation in
548 thermal inhalation injury. *Sci. Rep.* **2015**, 5, 15946.

549 49. Kim, M.; Ashida, H.; Ogawa, M.; Yoshikawa, Y.; Mimuro, H.; Sasakawa, C. Bacterial
550 interactions with the host epithelium. *Cell Host Microbe* **2010**, 8, 20-35.

551 50. Loncar, M.B.; Al-azzeh, E.D.; Sommer, P.S.; Marinovic, M.; Schmehl, K.; Kruschewski,
552 M.; Blin, N.; Stohwasser, R.; Gött, P.; Kayademir, T. Tumour necrosis factor alpha and
553 nuclear factor kappaB inhibit transcription of human TFF3 encoding a gastrointestinal
554 healing peptide. *Gut* **2003**, 52, 1297-1303.

 doi:10.20944/preprints201810.0144.v1

555 **Figure captions**

556 **Figure 1**. The Effect of EtCR on DSS-induced colitis. UC was induced by 5% DSS in the
557 drinking water for 7 days. During this period, EtCR (50 mg/kg) and 5-ASA (50 mg/kg) were
558 orally administrated once a day. **(A)** Body weight changes were measured. **(B)** Disease activity
559 index was investigated for the last 3 days. **(C)** The representative images of colon tissue were
560 shown. **(D)** Colon lengths were measured after sacrificing the mice. **(E)** Spleen weights were
561 measured. Values represent mean ± S.D. Data were analyzed by one-way ANOVA (#$p < 0.05$
562 vs. control, *$p < 0.05$ vs. DSS alone).

563

564 **Figure 2**. The Effect of EtCR on colon tissue damage and inflammation in colitis. **(A)**
565 Representative H&E staining images of colon tissue were observed by microscope
566 (magnification 100× and 200×). Scale bar = 200 μm. **(B)** Histological score was calculated as
567 described in materials and methods. **(C)** Colon tissues were stained with alcian blue
568 (magnification 100× and 200×). Scale bar = 200 μm. **(D)** Goblet cells stained with alcian blue
569 were counted. **(E)** The protein expressions (COX-2, iNOS, and TFF3) were determined by
570 western blot using colon tissue. **(F and G)** Relative protein levels were normalized to GAPDH
571 and measured using Image-J. Values represent mean ± S.D. Data were analyzed by one-way
572 ANOVA (#$p < 0.05$ vs. control, *$p < 0.05$ vs. DSS alone).

573

574 **Figure 3**. The Effect of EtCR on cytokines LPS-stimulated RAW 264.7 cells. Cells were pre-
575 treated with of EtCR for 1 h and then stimulated with LPS (200 ng/ml) for 24 h. **(A)**
576 Cytotoxicity of EtCR was measured using MTT assay. **(B-D)** Concentrations of IL-1β, TNF-α,

 doi:10.20944/preprints201810.0144.v1

and IL-6 were measured by ELISA kit using cell supernatants. Values are the mean ± S.D. Data were analyzed by one-way ANOVA (#p<0.05 vs. untreated cells, *p<0.05 vs. LPS-stimulated cells).

Figure 4. The Effect of EtCR on productions of NO and PGE_2 and the expressions of iNOS and COX-2 in LPS-stimulated RAW 264.7 cells. Cells were pre-treated with of EtCR for 1 h and then stimulated with LPS (200 ng/ml) for 24 h. **(A)** The amount of NO production was measured by the Nitrite Assay. **(B)** The amount of PGE_2 production was measured using the PGE_2 assay kit. **(C)** The expression of iNOS was determined by a western blot and band intensity was measured using Image-J. **(D)** The expression of COX-2 was determined by a western blot and band intensity was measured using Image-J. Values are the mean ± S.D. Data were analyzed by one-way ANOVA (#p<0.05 vs. untreated cells, *p<0.05 vs. LPS-stimulated cells).

Figure 5. The Effect of EtCR on NF-κB and MAPKs in LPS-stimulated RAW 264.7 cells. Cells were pre-treated with EtCR for 1 h, and then stimulated with 200 ng/ml of LPS for 30 min. The nuclear extracts were evaluated for NF-κB expression and cytosolic extracts were examined for IκB, p-IκB, and MAPKs expressions. **(A)** The expression levels of IκB, p-IκB, NF-κB, and PCNA were determined by western blot analysis. **(B)** Band intensities were normalized by GAPDH and PCNA using Image-J. **(C)** The NF-κB binding activity was determined by a NF-κB binding assay. **(D)** The expressions of p-JNK, JNK, p-ERK, ERK, p-p38, and p38 were determined by western blot analysis. **(E)** Intensities of p-JNK, p-ERK, and

 doi:10.20944/preprints201810.0144.v1

599 p-p38 were normalized by JNK, ERK, and p38, respectively and measured using Image-J.
600 Values are the mean ± S.D. Data were analyzed by one-way ANOVA (#p<0.05 vs. untreated
601 cells, *p<0.05 vs. LPS-stimulated cells).

602

603 **Figure 6**. The effect of EtCR on TFF3 in HT29 cells. **(A)** Cell viability was measured by MTT
604 assay. **(B)** The mRNA level of TFF3 was measured by real-time PCR. **(C)** The TFF3 expression
605 was determined by a western blot analysis. Band intensities were normalized by GAPDH and
606 were measured using Image-J. Values are the mean ± S.D. Data were analyzed by one-way
607 ANOVA (#p<0.05 vs. untreated cells, *p<0.05 vs. LPS-stimulated cells).

608

609

610

611

612

613

614

615

616

617

Preprints (www.preprints.org) | NOT PEER-REVIEWED | Posted: 8 October 2018 doi:10.20944/preprints201810.0144.v1

618 **Table 1**. Criteria for Disease Activity Index (DAI)

Score	Weight loss (%)	Stool consistency	Bloodstain or gross bleeding
0	None	Normal	Negative
1	1-5	Loose stool	Negative
2	5-10	Loose stool	Positive
3	10-15	Diarrhea	Positive
4	>15	Diarrhea	Gross bleeding

619

Preprints (www.preprints.org) | NOT PEER-REVIEWED | Posted: 8 October 2018 doi:10.20944/preprints201810.0144.v1

620 Figure 1.

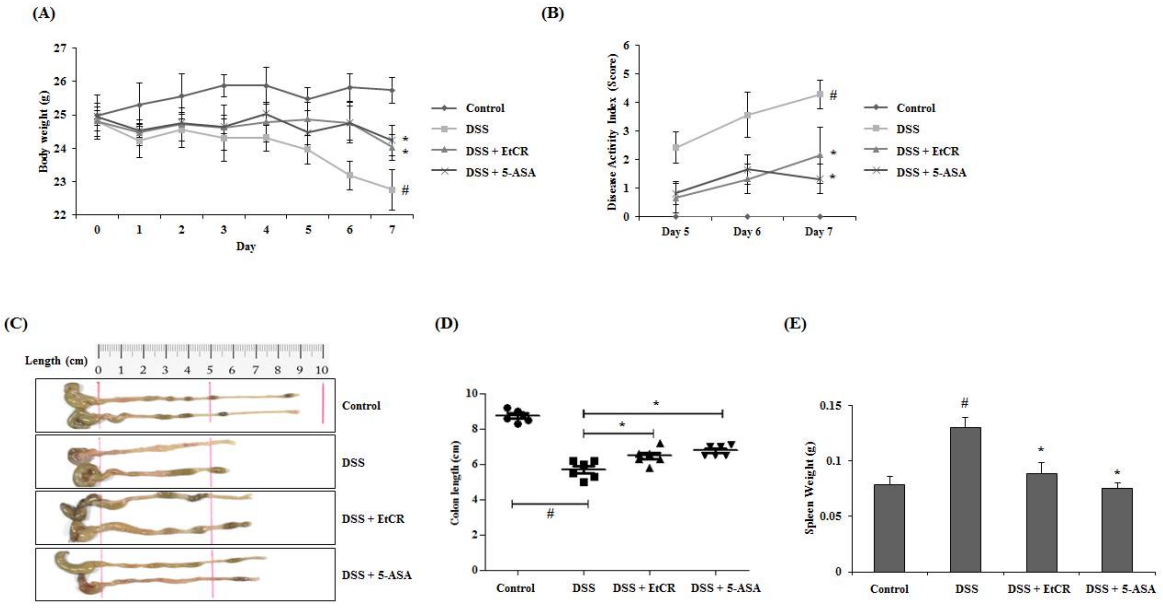

621

Preprints (www.preprints.org) | NOT PEER-REVIEWED | Posted: 8 October 2018 doi:10.20944/preprints201810.0144.v1

622 Figure 2.

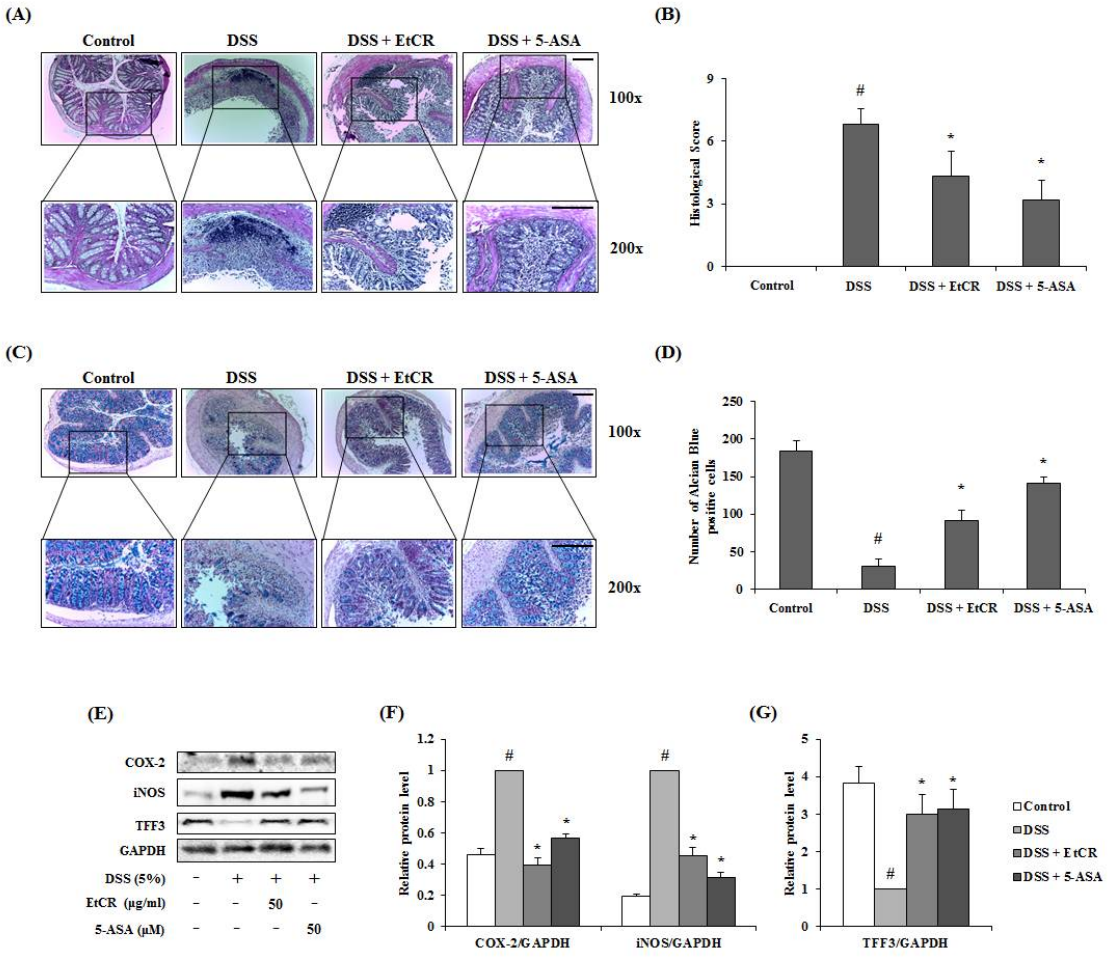

623

624

Preprints (www.preprints.org) | NOT PEER-REVIEWED | Posted: 8 October 2018 doi:10.20944/preprints201810.0144.v1

625 Figure 3.

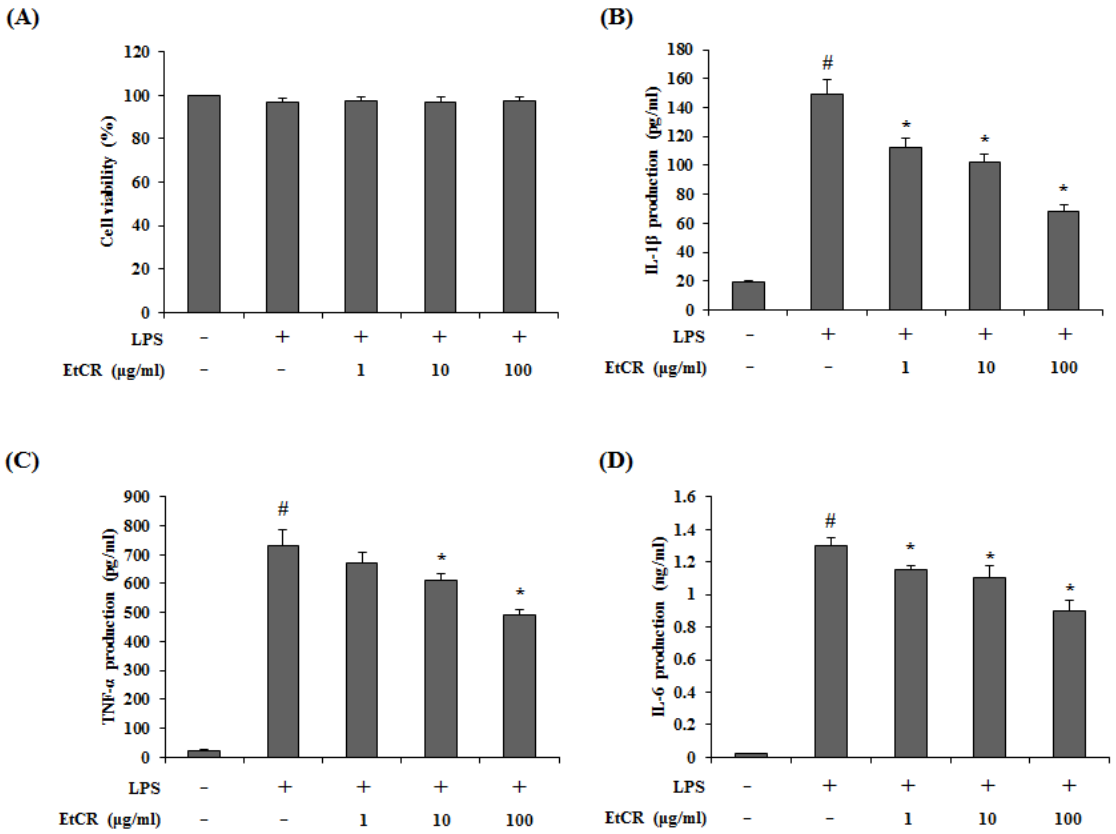

626

627

Preprints (www.preprints.org) | NOT PEER-REVIEWED | Posted: 8 October 2018 doi:10.20944/preprints201810.0144.v1

628 Figure 4.

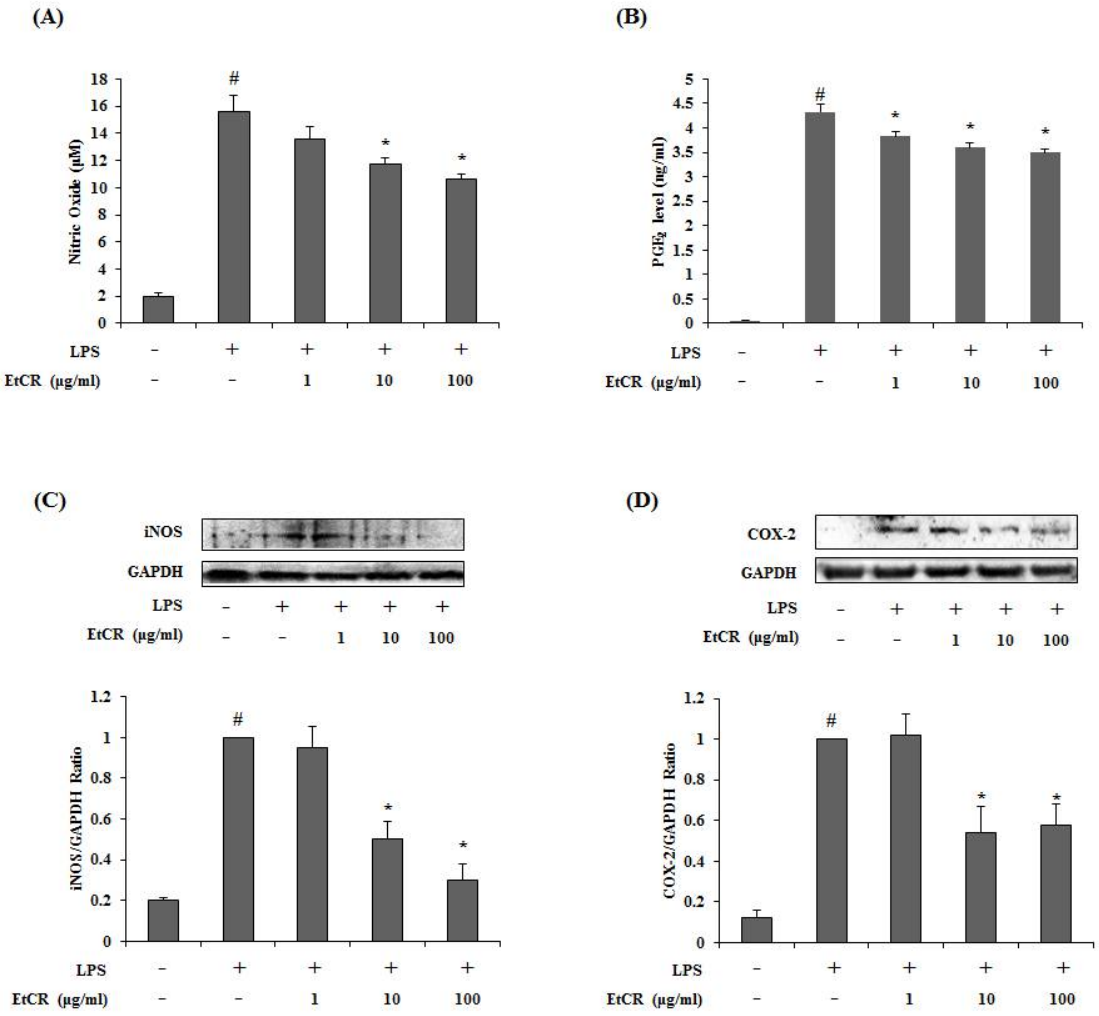

629

Preprints (www.preprints.org) | NOT PEER-REVIEWED | Posted: 8 October 2018 doi:10.20944/preprints201810.0144.v1

630 Figure 5.

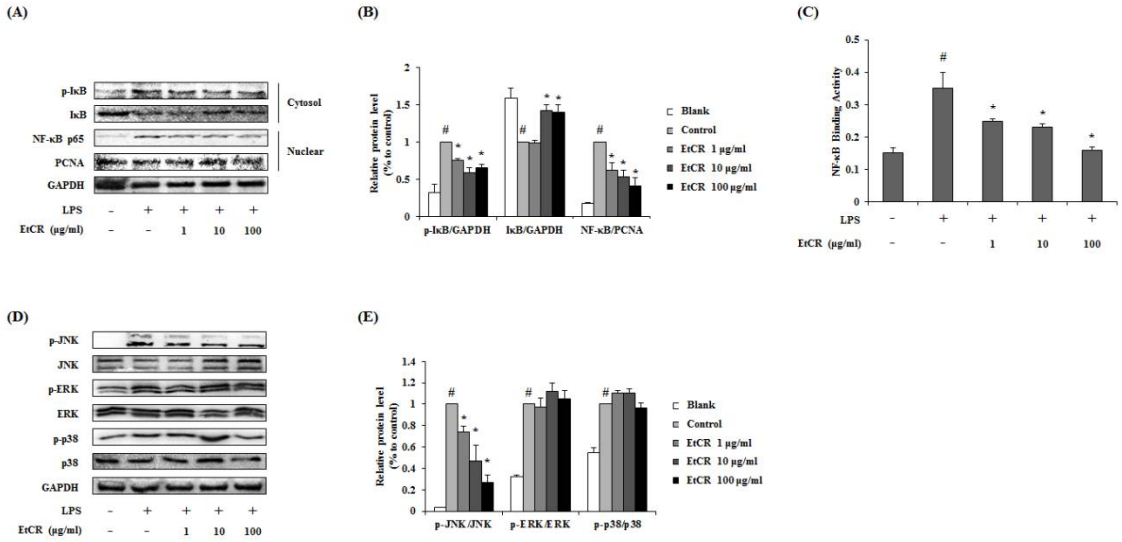

631

632

Preprints (www.preprints.org) | NOT PEER-REVIEWED | Posted: 8 October 2018 doi:10.20944/preprints201810.0144.v1

633 Figure 6.

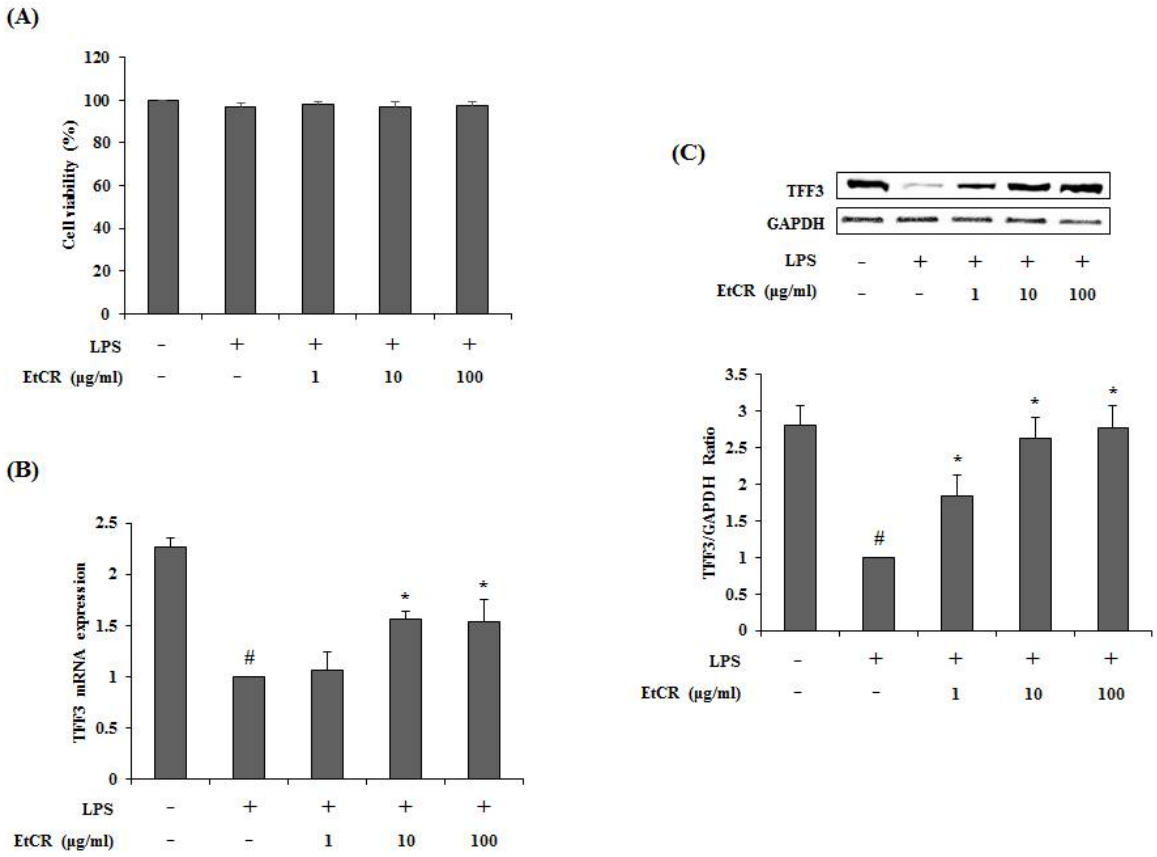

634

635

Preprints (www.preprints.org) | NOT PEER-REVIEWED | Posted: 8 October 2018 doi:10.20944/preprints201810.0144.v1

636 Graphical Abstract

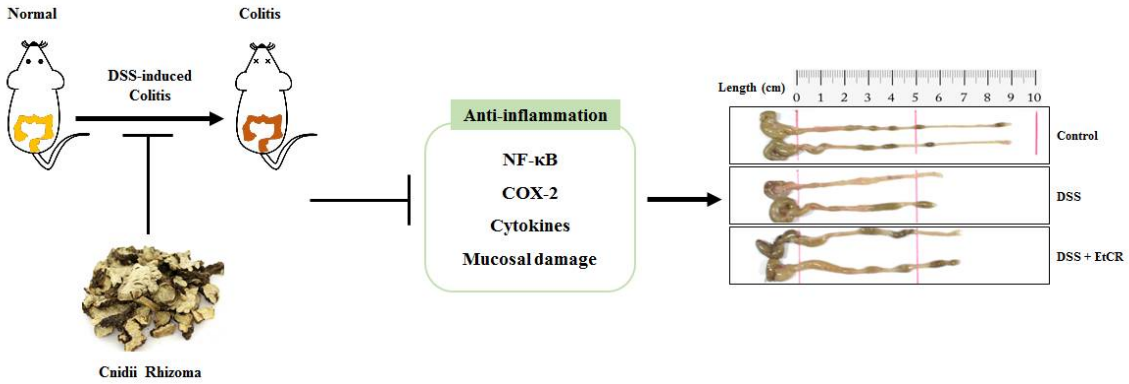

637